Eur Radiol (2006) 16: 1253–1269
DOI 10.1007/s00330-005-0103-3

Karl-Olof Lövblad
Alison E. Baird

Actual diagnostic approach to the acute stroke patient

Received: 16 August 2005
Revised: 18 November 2005
Accepted: 25 November 2005
Published online: 22 December 2005

K.-O. Lövblad (✉)
Neuroradiology Unit,
Radiology Department, SRRI,
HUG Geneva University Hospital,
24 rue Micheli-du-Crest,
1211 Geneva 14, Switzerland
e-mail: karl-olof.lovblad@hcuge.ch
Tel.: +41-22-3727033
Fax: +41-22-3727072

A. E. Baird
Stroke Neuroscience Unit, NiNDS,
Bethesda, MD, USA

Abstract Since acute stroke is now considered a potentially treatable medical emergency, a rapid and correct diagnosis must be made. The first step is to exclude hemorrhage, then to visualize any early ischemic changes, demonstrate the presence of hypoperfusion and locate the presence of a vascular underlying pathology as well as elucidate the presence of a potential penumbra (tissue at risk). Thanks to improvements and advances in both MR and CT technology, this can now be done in a number of ways. At the moment, CT is the most widely available and fast method for obtaining imaging of the brain and neck vessels of patients presenting with acute stroke. MRI can provide more precise information, although it remains slightly more time-consuming, but is, however, the method of choice for follow-up imaging. The main point is to take the one-stop-shopping approach where imaging of the vessels and brain is done from the aortic arch to the circle of Willis in one single session in order to have all the necessary information in the acute phase.

Keywords Stroke · Computed tomography · Magnetic resonance imaging · Penumbra · Diffusion imaging

Introduction

Imaging and acute stroke

Until 10 years ago, stroke was considered a hopeless disease for the patients it affected, who would spend their life with major handicaps or in extensive rehabilitation programs. Therefore, there was no need for imaging to provide any detailed information about the parenchyma and vessels in the acute stage, but was mainly used to demonstrate hemorrhage or for follow-up of intracerebral lesions. This was the case until the first positive study on the use of rTPA in stroke was performed and showed improvement when patients were treated acutely intravenously [1]. This pioneering study was partly reproduced by the ECASS studies [2, 3], but less spectacularly, and mainly by demonstrating that stroke could be approached as a treatable disease. It opened the way for groups to study further possibilities such as intra-arterial thrombolysis using other thrombolytics such as urokinase [4–6] or recently even mechanical thrombus extraction [7, 8]. Indeed, evidence points to the advantage of also treating the clot itself more directly. All these advances have thus prompted the need for improved imaging at all the levels of the brain and neurovascular tree.

Thus, in order to optimize treatment, even in the acute phase, it is of prime importance to perform a complete neurovascular imaging session in one go, adopting the one-stop shopping approach where imaging of the vessels and brain is done from the aortic arch to the circle of Willis; this will provide the radiologist and the clinician with the complete picture needed in order to start treatment (Figs. 1 and 2). Indeed, it is not simply important to see whether something has happened at the level of the brain, but also to localize the level of the vascular pathology that is causing it, be it at the level of the circle of Willis, the cervical carotids or even the aortic arch (and even as low as in the left ventricle of the heart). Due to advances in Gd-MRA

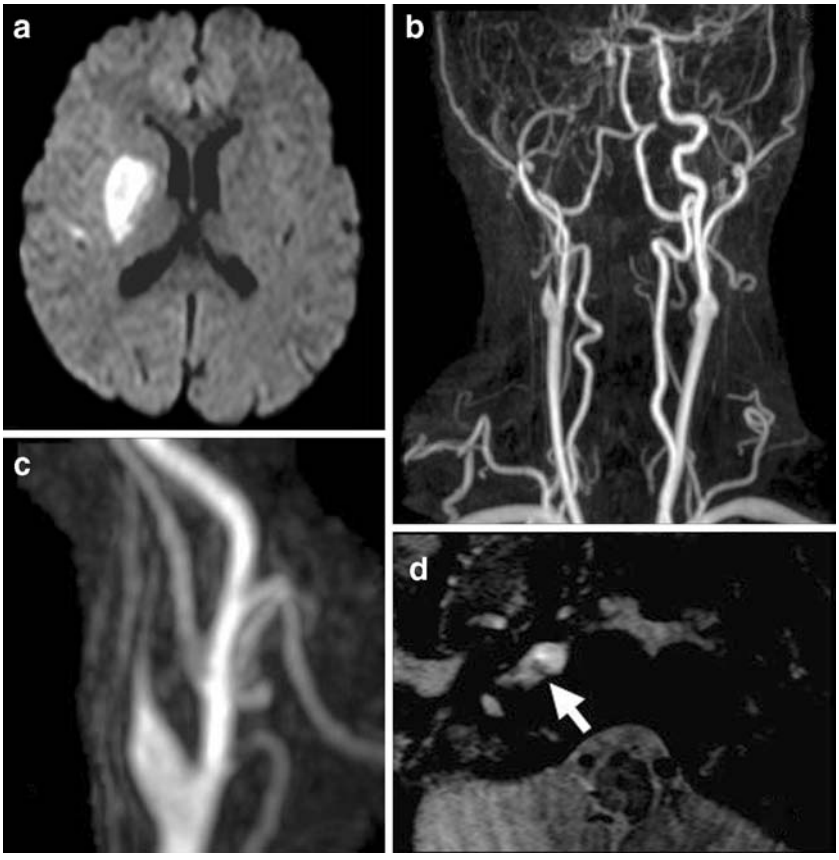

Fig. 1 MRI all-in-one approach in a patient with right-sided carotid dissection. The diffusion-weighted image shows a hyperintense lesion in the basal ganglia (**a**). The Gd-MRA (**b**) of the whole carotid system demonstrates an occlusion of the right carotid after the bifurcation and the rotated image shows a typical tapering of the carotid lumen (**c**), indicative of a dissection. In the petrous portion of the carotid, there is hyperintensity instead of the flow void (*arrow*)

and CT angiography techniques, this is now unproblematic with both modalities. It is thus possible to determine the type of stroke [9] and its possible cause [10]. Indeed, while atherosclerosis is the most common type of cause, other causes may occur that have different treatments such as arterial dissection, small vessel disease, inflammatory and non-inflammatory vasculopathy and vasomotor disorders [10]. Also, the stroke itself may be classified into various groups either due to anatomic localization or etiologies [9].

Exclusion of hemorrhage

Indeed, since we are considering using thrombolysis, it is imperative to at first exclude intracerebral hemorrhage. This was done for a long time because CT in general was easier to perform in the setting of stroke. Due to the development of standardized MR imaging protocols with diffusion imaging [11–13], MRA and susceptibility imaging, it has become possible to image the possibly ischemic brain within an acceptable timeframe (i.e., less than 20 min). In clinical practice the exclusion and demonstration of hemorrhage can still be best done by CT, even though MRI has been shown by many authors to be able to detect acute bleeding by using a combination of sequences [14–16], mainly gradient echo sequences and even diffusion-weighted imaging using echo-planar technology. Indeed, MRI should in theory be more sensitive to hemorrhagic changes [17–19], but the findings are often somewhat confusing to the non-initiated clinician. While MRI can be used to demonstrate hemispheric hemorrhage (Fig. 3), its utility in demonstrating more subtle blood as found in subarachnoid hemorrhage still has to be demonstrated clinically (Fig. 4). CT, however, has been used in the main published trials since it remains easier to use and to interpret when facing the possibility of the occurrence of acute hemorrhage. Recent studies such as that of Nighogossian have shown that the use of T2* images can detect microbleeds indicative of potential hemorrhage [20].

Demonstration of ischemic lesions

Computed tomography

Computed tomography signs of acute early cerebral ischemia are well known and established [21, 22]. These arise mainly from the presence of early edema. This edema will lead to hypodensity (Fig. 5) and to a diminished distinction of white and grey matter structures: loss of clear visualization of the insular ribbon (Fig. 6) and lenticular nucleus (Fig. 7) as well as the loss of cortical differentiation (Fig. 8). The sign that is the most important to recognize is the presence or absence of early edema, since this very

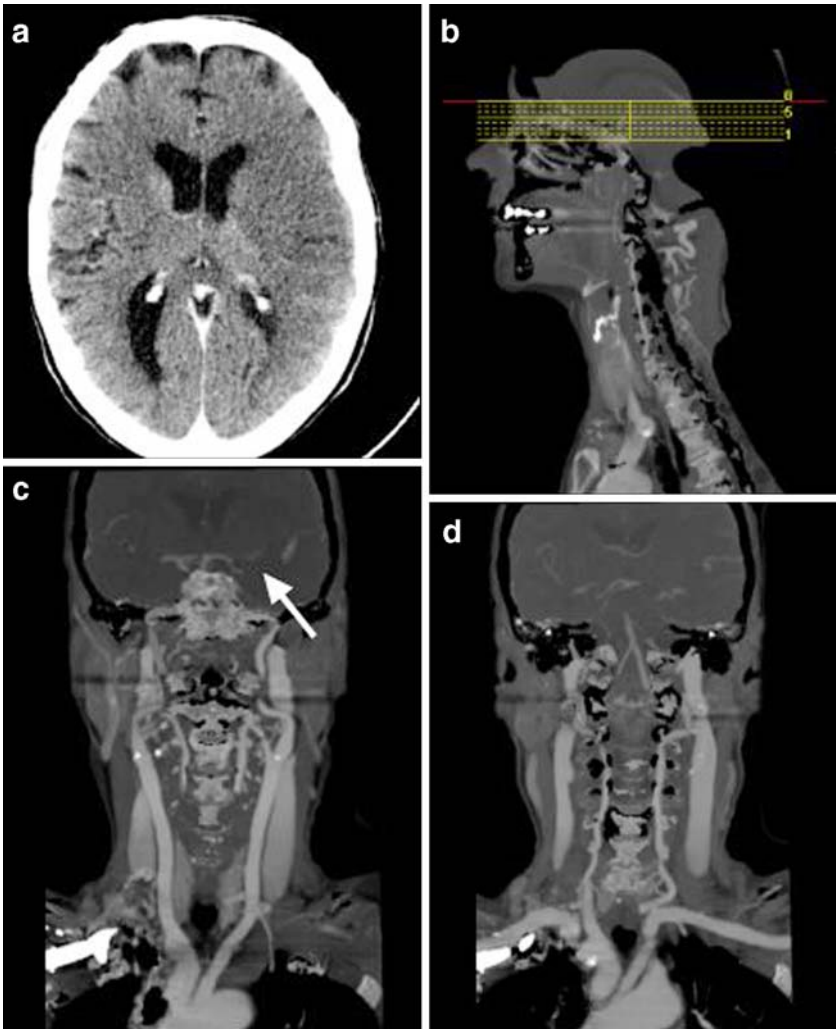

Fig. 2 Multimodality CT in a patient with acute left hemispheric stroke. There is beginning hypodensity with mass effect in the left MCA territory (**a**). The angio-CT is reconstructed in the sagittal and coronal planes (**b**–**d**). The coronal reconstruction shows an occlusion of the M1 segment on the left (*arrow*) (**c**)

often has therapeutic impact. These signs have been demonstrated to be well recognizable by trained physicians [23, 24]. Beginning hypodensity corresponding to decreased X-ray absorption by the tissue corresponds to water accumulation. When this early hypodensity is visible in more than 30% of the affected MCA territory, there is an increased risk of secondary bleeding if thrombolysis is started; this was an important finding of the ECAS study [25, 26] (Fig. 9).

Also of diagnostic importance is the presence of dense arteries, signifying acute occlusion: this sign will be found at any location, but is most easily recognized at the level of the MCA or the basilar artery [27, 28]. At the level of the MCA, this sign has been recognized in approximately 40% of cases. Gadda et al. have found it to be a predictor of a more restricted extension of the infarct using multidetector CT images [29]. Some false-positive situations such as hyperviscosity, high erythrocyte counts, vascular calcification and childhood are important to know (Figs. 10 and 11).

Magnetic resonance imaging

While conventional magnetic resonance imaging, especially T2-weighted imaging, is not very sensitive to the changes associated with ischemia before 8 to 12 h [30–33], it was the development of newer and more robust diffusion and perfusion sequences that allowed MRI to enter the clinical arena of stroke neurology. This was due to the development of clinically available echo-planar scanners, capable of scanning the whole brain in less than a second [34]. Thus, diffusion and perfusion MR techniques were made available that could quickly image patients with a clinical suspicion of stroke. Diffusion imaging was developed by Le Bihan and consists of a spin-echo sequence that is modified to be sensitive to tissue motion [35]. In acute stroke, the sequence of events of the ischemic cascade leads to an early local water shift from the extra- to intracellular compartments (without a global water increase initially: hence the normal T2-weighted images), which

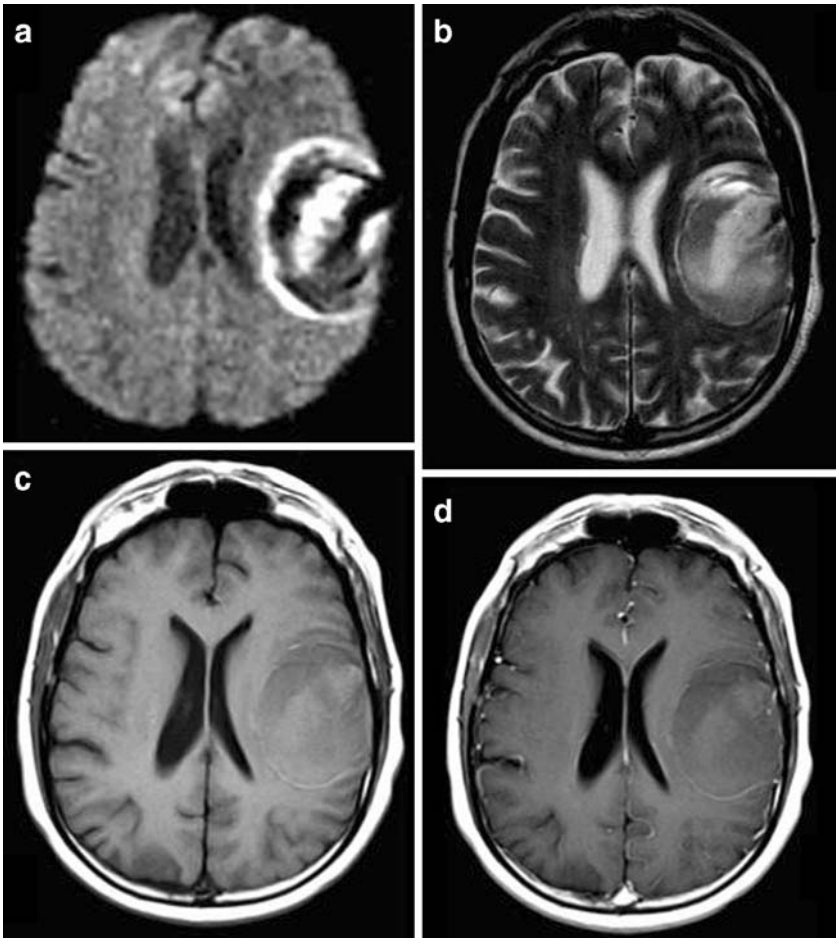

Fig. 3 Patient with acute lobar hemorrhage: the DWI image shows a mass lesion in the left frontal lobe (**a**) that is inhomogeneous with both hypo- and hyperdense areas. The T2-weighted image shows a defined lesion that is slightly hyperintense (**b**), whereas on T1-weighted images it is isointense (**c**) and does not enhance (**d**)

causes a decrease in the diffusion (and apparent diffusion coefficient), which is reflected in an increased signal on the diffusion-weighted image with the maximal *b* value (usually 1,000) [36] (Fig. 12). The first clinical applications were performed by Warach and Chien and used as the first clinical scanners with slower sequences that were more prone to motion-induced artifacts [37, 38], but later on echo-planar imaging allowed whole-brain imaging studies to be performed routinely [39, 40]. Diffusion imaging thus provides images of acute stroke with a high sensibility and specificity, as was shown by Lövblad et al. [41] and Gonzales et al. [42]. Reports on humans have shown them to occur within 1 h. Indeed, one of the earliest reports shows DWI to be positive 39 min after the onset of symptoms [43]. We have also observed this to occur in random cases where the ischemic event occurred in the hospital in the presence of a physician who was able to report the exact start of events. This has allowed people to compare the diffusion hyperintensity to the early ECG signs in cardiac stroke [44]. In the largest study of patients studied with DWI in stroke, Lövblad et al. found that diffusion-weighted MR imaging studies were positive in 133 of 151 cases of infarction (88% sensitivity) and negative in 41 of 43 cases with no infarction (95% specificity) [41]. Two cases identified as positive on diffusion-weighted images had non-ischemic diagnoses (1.5% false-positive rate). Diffusion-weighted imaging had a positive predictive value of 98.5% and a negative predictive value of 69.5%. Use of T2-weighted sequences as well as diffusion-weighted imaging produced no false-positive findings. Of the negative scans, 69.5% corresponded to transient ischemic attacks or infarcts (mostly small brain stem infarcts). When only cases scanned within 6 h of onset were considered, the sensitivity rose to 94% and the specificity to 100%. When imaging patients within 6 h, Gonzalez et al. found 100% sensitivity and 86% specificity for diffusion-weighted MR imaging [42]. Further expanding this series, they found that, in the diagnosis of stroke in the early period (<12 h after presentation), DWI is superior to conventional MR imaging and CT [45] (Fig. 13) and due to its higher capacity to detect lesions may also help in differentiating hemodynamic strokes from embolic strokes. Indeed, very often hemodynamic lesions will have a typical "string of pearls" appearance with multiple lesions located in the typical watershed areas (Fig. 14).

Diffusion techniques have also been shown to be superior to plain CT in a series of papers [46, 47], but these findings still need to be validated. MR imaging is clearly indicated to perform the follow-up of patients, especially when recanalization has been performed, since ADC

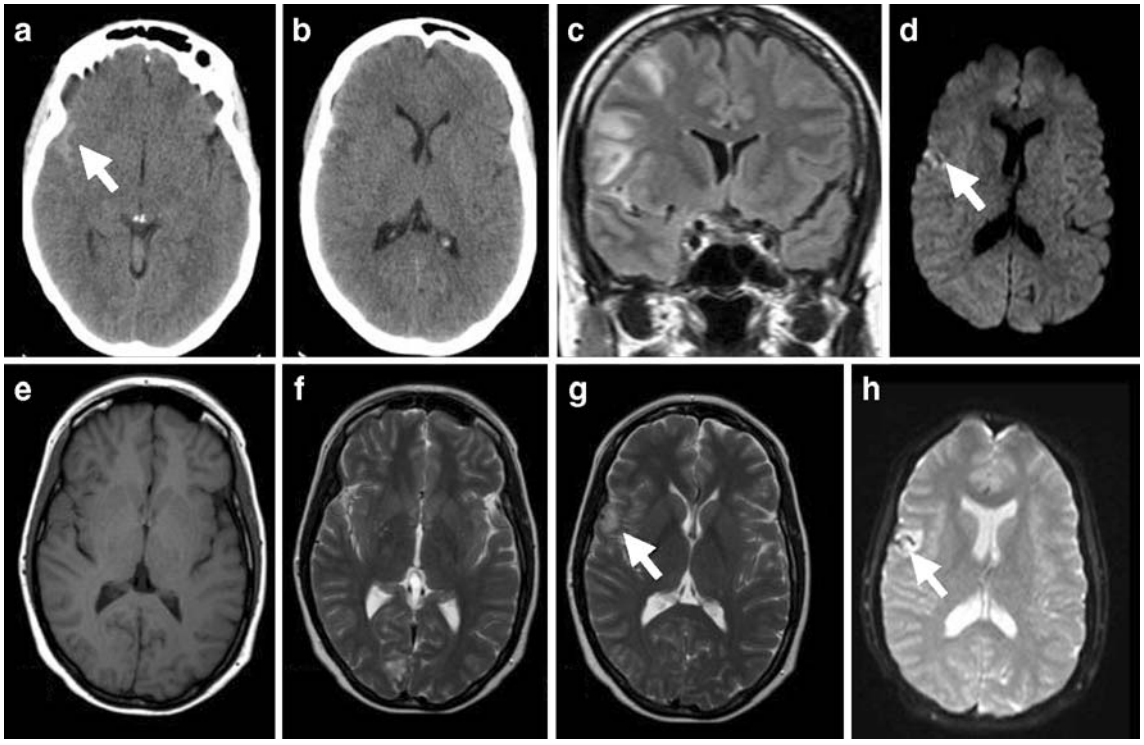

Fig. 4 Acute subarachnoid hemorrhage: CT (**a**, **b**) shows hyperdensity in the right sylvian fissure (*arrow*). On the FLAIR images, there are hyperintensities in the sulci on the surface of the right frontal lobe (**c**). On DWI there is also a sylvian hyperintensity (*arrow*) (**d**). On T2- and T2*-weighted images there are also areas of perturbed signal (*arrows*) (**g**, **h**)

values can show the depth and extent of the ischemia [48]. This has been useful since DWI lesions have been shown to diminish and the ADC values to revert partially or completely to normal following therapy, in agreement with previous animal data [48–53]. Some authors have even further demonstrated that the ADC can predict clinical outcome, i.e., the lower the ADC, the worse the clinical outcome, as shown by Oppenheim et al. in their studies [54, 55].

Venous ischemia

While more frequent and less mortal than has been initially thought, venous cerebral occlusive disease is sometimes very difficult to diagnose in the early stage. Computed tomography is superior to magnetic resonance imaging since CT venography corresponds more exactly to digital subtraction venography [56]. Magnetic resonance techniques such as contrast-enhanced MR phlebography may more reliably demonstrate cortical venous thromboses and is also suggested for follow-up due to the lack of radiation [57]. Also diffusion and perfusion techniques provided by MRI can deliver more information about the integrity of the surrounding cerebral tissue [58] (Fig. 15).

False-negative imaging and stroke-mimicking syndromes

Whenever confronted with a patient who has acute negative imaging, it is important to perform a second imaging study, very often MRI, to determine whether we are dealing with a patient with a pathology mimicking stroke or not.

False DWI negatives and positives

Magnetic resonance and diffusion-weighted MRI may be normal in stroke-like syndromes [59] and may even under certain circumstances be normal in strokes [60]. In transient ischemic attacks, diffusion MRI demonstrates ischemic abnormalities in nearly half of the clinically defined TIA patients [61] (Fig. 16); this has a relatively important implication since it means that these patients did not suffer from hemodynamic symptoms, but from a stroke with

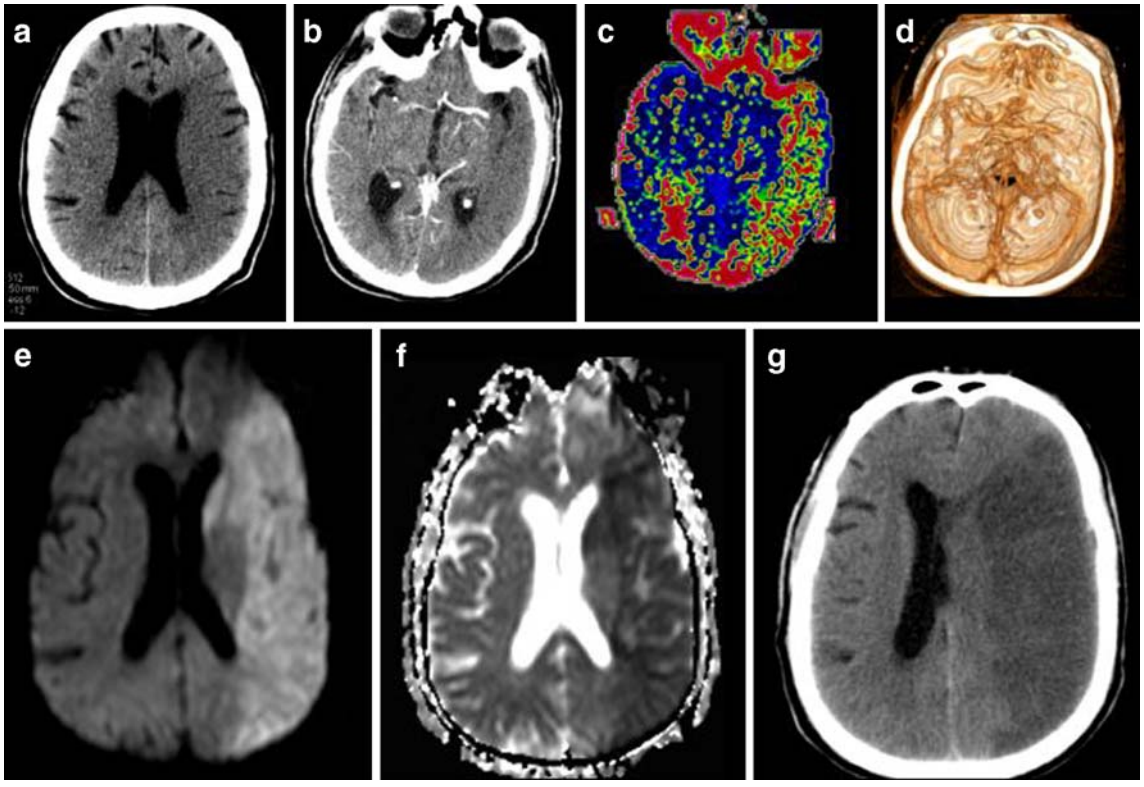

Fig. 5 Acute CT showing slight hypodensity in the left MCA territory (**a**). The raw angio-CT source images show occlusion of the left MCA (**b**). The perfusion CT shows significantly decreased perfusion in the left MCA territory (**c**), corresponding to the occlusion of the distal M1 segment seen on the reconstructed angio-CT (**d**). Follow-up MRI shows hyperintensity on the DWI image (**e**) and hypodensity on the ADC (**f**), corresponding to acute infarction. Follow-up CT demonstrates progression of edema and beginning of herniation of the midline (**g**)

transient symptoms. This will mean that the patient might benefit from the same treatment as a patient with a large hemispheric stroke (i.e., thrombolysis).

Stroke mimics

The aim of imaging is not just to include into therapy any patient who has no hemorrhage and a DWI hyperintensity,

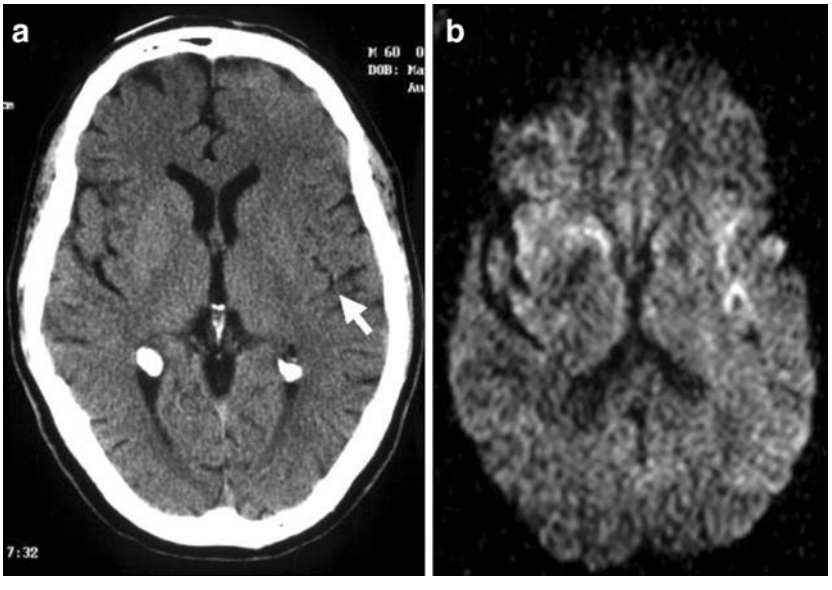

Fig. 6 Patient with clinical symptoms of stroke for 2 h. Effacement of the insular ribbon in the left hemisphere (*arrow*) (**a**). There is also discrete sulcal effacement. On the DWI image there is a slight hyperintensity in the left insular region (**b**)

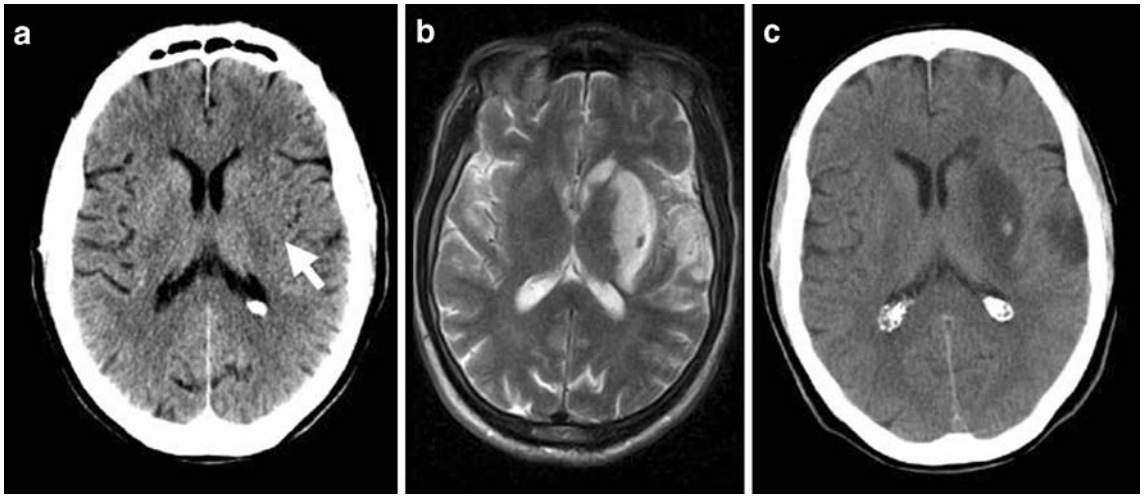

Fig. 7 Patient with acute stroke of 1.5 h onset: the acute CT shows disappearance of the left-sided lenticular nuceus (*arrow*) (**a**). On the follow-up MRI (**b**) and CT (**c**) there is an ischemic lesion with hemorrhagic inclusions (hypointense on MRI, hyperdense on CT)

but also to detect some stroke-like situations that might look like a cerebrovascular event. This is an area of clinical neuroimaging where MRI is clearly superior to CT. A few pathologies exist that closely resemble a stroke on DWI, namely infectious diseases and epilepsy.

Concerning epilepsy, diffusion imaging is sensitive to the changes observed in epilepsy. In the chronic phase, there are very discrete changes that can be observed in the ADC, whereas in the case of patients with status epilepticus, hyperintensities have been observed in the affected cortex. This corresponds well to what has been observed in experimental models of epilepsy and to what has been observed in cases of well-documented experimental spreading depression. Indeed, in spreading depression, waves of ADC reductions have been seen in the cortex corresponding to waves of depolarizations. Thus, DWI is very sensitive to neurophysiologic changes occurring in the cortex. However, in the acute phase these DWI hyperintensities are accompanied by hyperperfusion and not hypoperfusion as in stroke [62]. This supports the validity of ADC measurements in acute stroke, which despite some controversy seem related to tissue outcome.

Demonstration of underlying hypoperfusion

This is done by perfusion imaging, performed either with MRI or CT technology.

MR imaging

The advent of fast imaging techniques such as echo-planar imaging and/or gradient-echo imaging has allowed us to

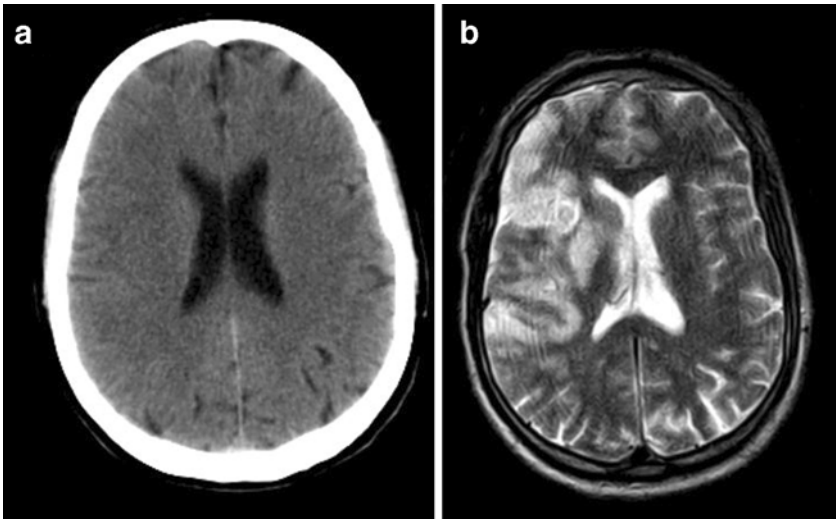

Fig. 8 Patient with acute right-hemispheric stroke of 2.5 h onset. Sulcal effacement over the right hemisphere on acute CT (**a**). On follow-up MR 2 days later there is a large area of the right MCA territory that is infarcted (**b**)

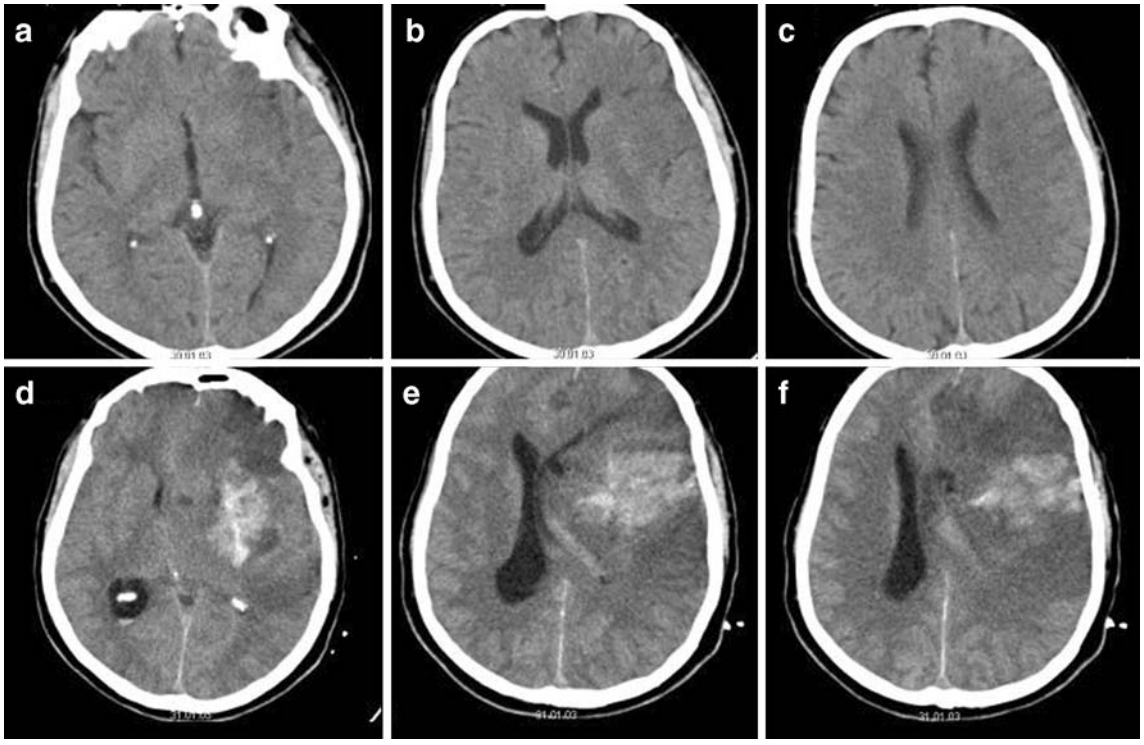

Fig. 9 Beginning hypodensity and mass effect in the left MCA territory (**a**–**c**). The hypodensity corresponds to more than 33% of the territory. After thrombolysis, the next day there is massive hemispheric bleeding and brain herniation (**d**–**f**)

acquire MR images quickly and repeatedly that are sensitive to changes induced by contrast materials [63]. Perfusion of the brain with MRI is done principally with three techniques: contrast-enhanced techniques [64–66], arterial spin-labeling techniques [67] and the BOLD principle. The BOLD technique is mainly used in func-

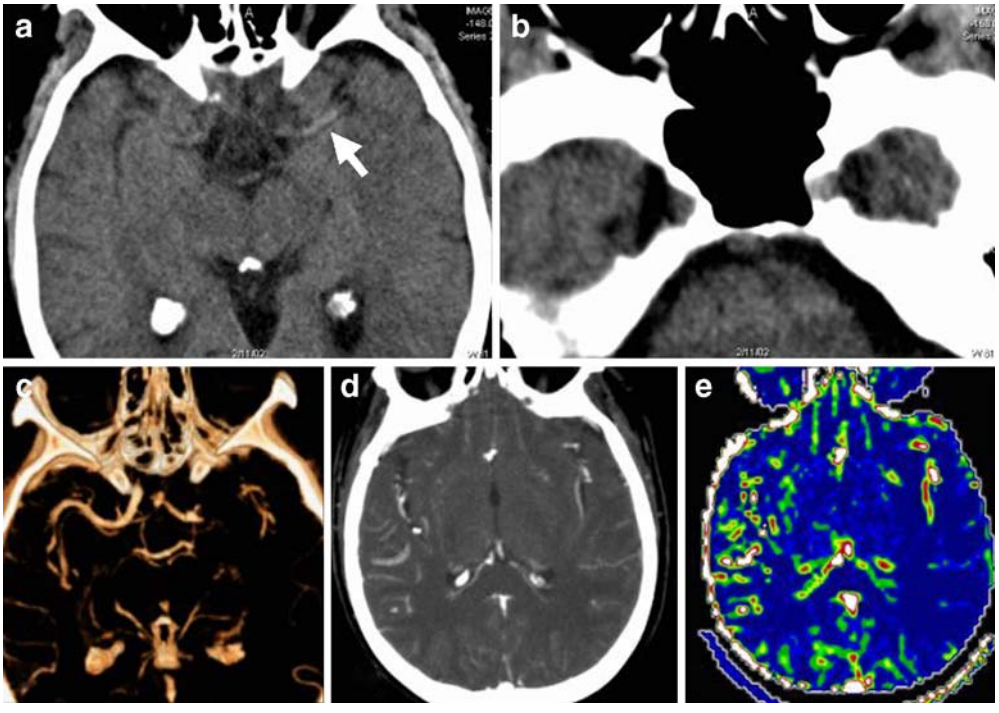

Fig. 10 Patient with left hemispheric stroke: on the unenhanced CT iamges there is a hyperdensity of the MCA (**a**) and the terminal portion of the internal carotid artery (**b**), which corresponds to occlusion. This occlusion is seen on the angio-CT with corresponding deep hypoperfusion of the left hemisphere

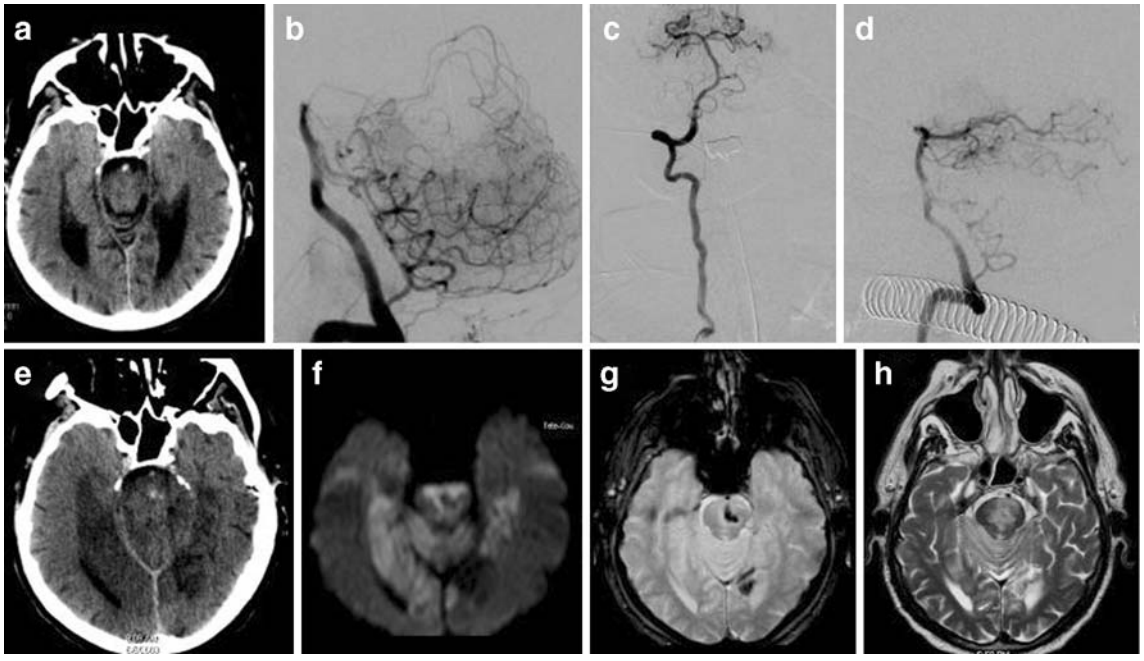

Fig. 11 Patient with progressive coma: on unenhanced CT there is a hyperdense basilar artery (**a**). The occlusion of the basilar artery is confirmed on angiography with a stop at the end of the basilar artery (**b**), while angiographic reperfusion is good after local intra-arterial thrombolysis (**c**) with visualization of the posterior cerebral arteries (**d**); the next day there is progressive ischemia in the posterior fossa (**e**) with hemorrhagic transformation already visible on CT, but better seen on MRI (**f**–**h**)

tional activation imaging and has been used in stroke [68, 69]. The problem with contrast-derived MR perfusion techniques is that one measures variations in the magnetic field that represent extreme susceptibility artifacts, rendering quantification difficult (e.g., the measurement of CBV and CBF). Also, we are mainly using relative values, since no reliable arterial input function is obtained. Studying various parameters from T2* imaging, Sorensen found that lesion volumes on blood volume and diffusion maps correlated better with eventual infarct volumes than did those on blood flow and tracer mean transit time maps [70]. T1-weighted MR perfusion imaging is possible and probably advantageous, but it has not yet established itself as a viable option [71].

However, the use of PWI in addition to DWI has allowed Steven Warach [72], among others, to develop a model of penumbra that can be used in clinical practice. The central area of diffusion anomaly at the first time point corre-

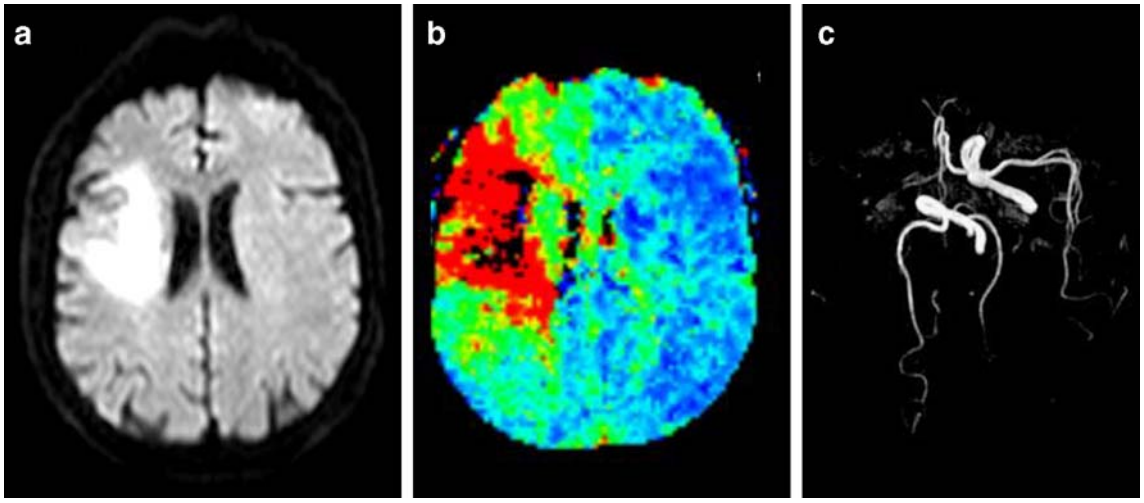

Fig. 12 Operational definition of the penumbra: in this patient with an acute right-hemispheric stroke there is a large DWI hyperintensity (**a**) surrounded by a larger area of hypoperfusion (**b**). This area is the potential penumbra. Angio-MR revealed a carotid occlusion (**c**)

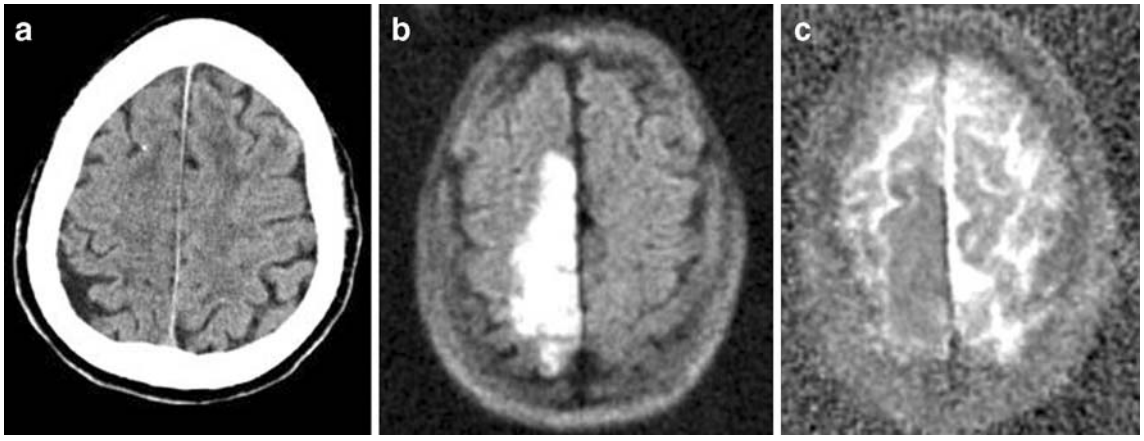

Fig. 13 CT vs. MRI in acute stroke: CT done on admission shows slight sulcal effacement in the right frontal lobe (**a**). MRI was performed right afterwards, and on DWI there is a clearly visible hyperintensity (**b**), seen as a hypointensity on the ADC map (**c**)

sponds to the ischemic core, while the hypoperfused area surrounding it represents the penumbra, or tissue at risk of undergoing further infarction if nothing is undertaken. This model has been proven usable clinically by many authors since then.

CT

Recently, much emphasis has been placed on the use of CT perfusion techniques for the acquisition of cerebral perfusion maps, even at low injection rates [73]. Wintermark et al., after having validated perfusion CT in stroke with

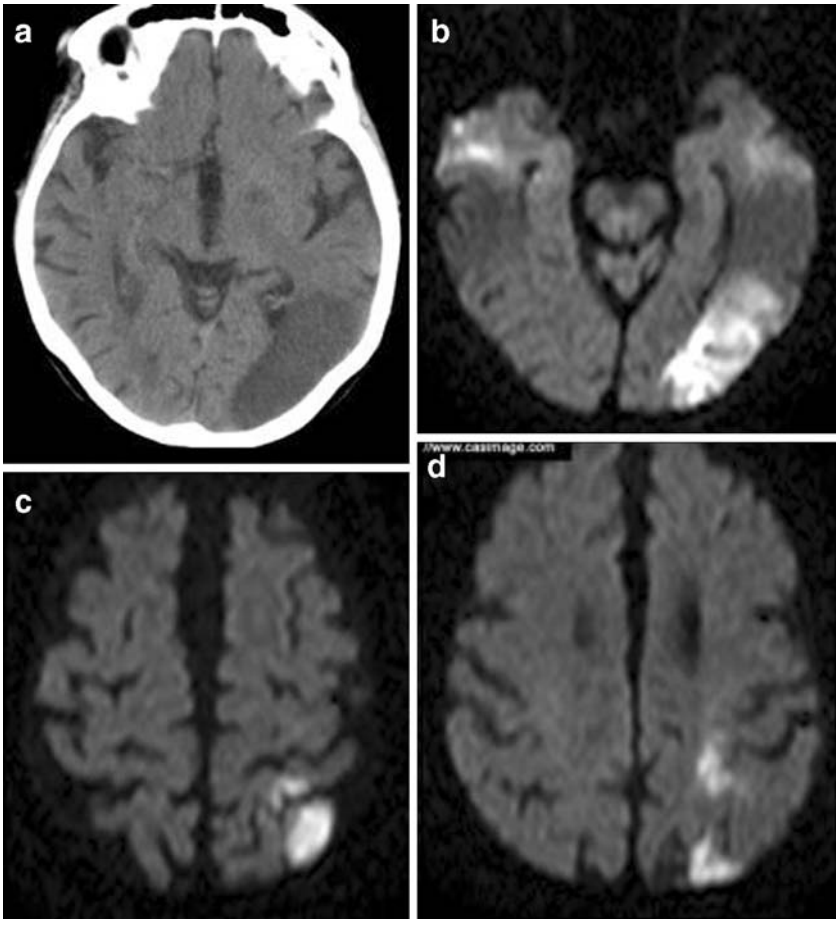

Fig. 14 Patient with hemodynamic stroke due to stenosis: on CT there is a hypodensity in the right-sided occipital lobe (**a**). On the DW images one can see multiple lesions (**b**–**d**) arranged in a string-of-pearls fashion in the watershed areas over the surface of the brain

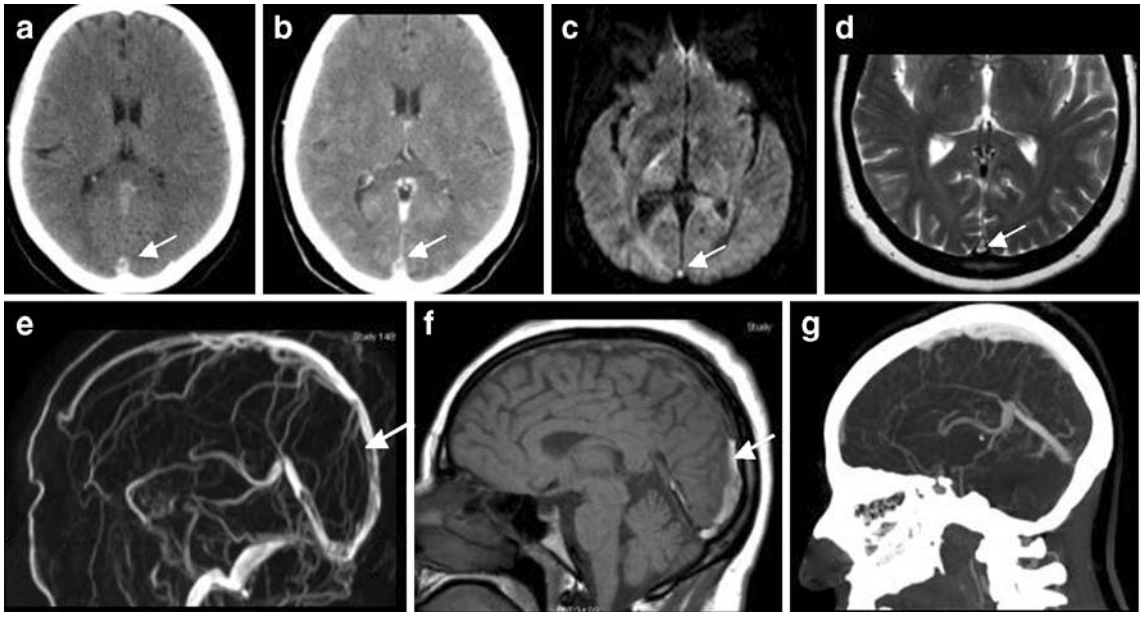

Fig. 15 Patient with thrombosis of the superior sagittal sinus (*SSS*): on unenhanced CT the SSS is prominent and spontaneously hyperdens (**a**). After contrast administration there is a so-called empty triangle or delta sign (**b**). On DWI the thrombus is hyperintense (**c**), and is also hyperintense on T2-weighted images (**d**). The MR venography demonstrates irregularity of the posterior portion of the SSS (**e**), seen on the sagittal T1-weighted image (**f**), as well as on the CT venogram (**g**)

Xenon CT [74], showed that it is possible to acquire dynamic perfusion CT (PCT) with deconvolution, which produces maps of time to peak (TTP), mean transit time (MTT), regional cerebral blood flow (rCBF), and regional cerebral blood volume (rCBV), with a computerized automated map of the infarct and penumbra. They found that dynamic perfusion CT maps are more accurate than non-enhanced CT in detecting hemispheric strokes. However, perfusion CT still has a limited spatial coverage, which should be overcome with more detector arrays [75], since new generations of CT units have up to 64 arrays.

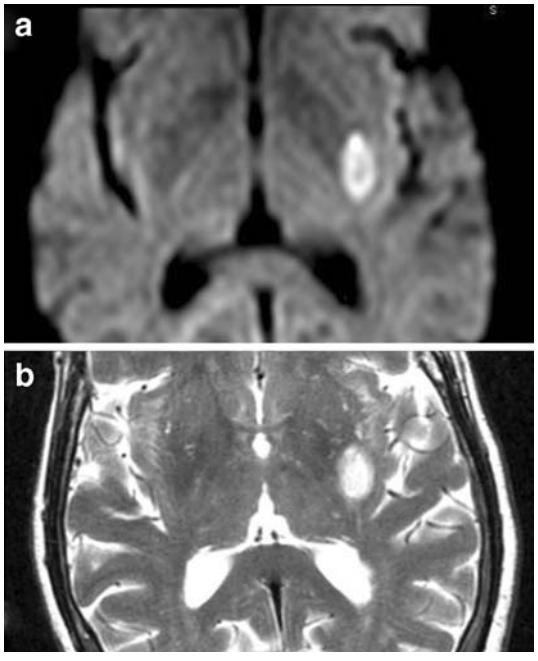

Fig. 16 Patient with transient right-sided symptoms, mimicking a transient ischemic attack. In this case the initial DWI shows a lesion in the left striatum (**a**), whose edema compresses the posterior limb of the internal capsule

Demonstration of underlying vascular pathology

While conventional, or nowadays digital subtraction angiography remains the gold standard for the demonstration of any vascular pathology, including occlusion, it cannot be performed routinely in all cases with suspected strokes, partly because of the radiation exposure, duration of the examination and also because it is not available everywhere where the diagnosis and treatment are initiated. Besides the dense artery signs described above that are indirect signs of vascular occlusion on plain CT, the direct demonstration of vascular pathology necessitates either angio-CT or MR angiography; indeed, both of these techniques now permit the visualization of the vascular tree from the aortic arch to the circle of Willis. Angio-MRI is usually performed in two stages: first a 3-D time-of-flight sequence is performed for the intracranial vasculature because of its high spatial resolution and then a contrast-enhanced MR sequence is performed [76]. This sequence is a dynamic fast sequence that provides a robust luminography of the examined vessels. Remonda et al. in a series of 120 patients have demonstrated that the grading of

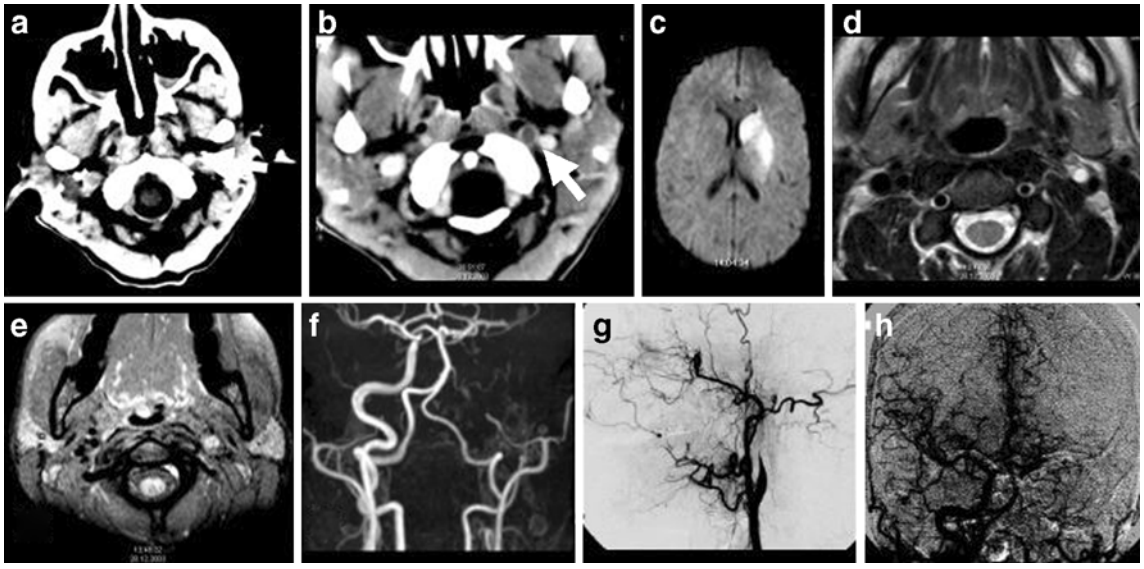

Fig. 17 Patient with left-sided carotid dissection. On non-enhanced CT there is a slight hyperdensity of the left carotid artery in the distal cervical segment (*arrow*) (**a**). After contrast injection there is no enhancement of the occluded carotid (**b**). DWI shows ischemia in the left basal ganglia (**c**). On T2-weighted images there are no flow voids in the carotid lumen (**d**), and there is hyperintensity as well on the T1-weighted images with fat suppression (**e**). MRA shows the occlusion of the left carotid (**f**). Angiography shows the typical tapering of the carotid lumen (**g**), and parenchymography reveals a perfusion deficit over the left hemisphere (**h**)

stenoses on Gd-enhanced MR angiograms agreed with the grading of stenoses on DSA images in 89% of arteries [77]. CT angiography (CTA) has improved technically so that it is easily feasible using deconvolution techniques that allow both CTA and perfusion studies within one simple imaging protocol. Indeed, Sims et al. in a study of 47 patients with acute MCA occlusion found that patients with patent vasculature or occult distal occlusion on CTA before treatment have a better clinical outcome as well as better chances of early improvement and early independence with fewer

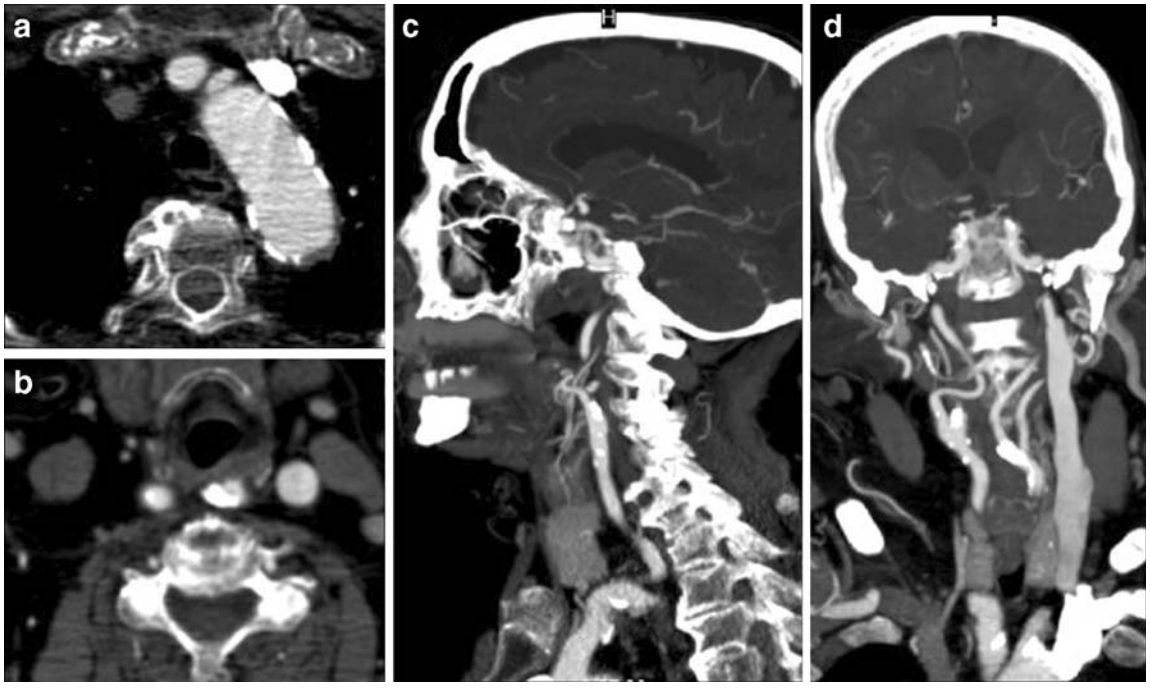

Fig. 18 Massive calcification at the level of the aorta (**a**) and carotids (**b**–**d**) seen on this CT examination that covers the upper thoracic and neck regions (**c**, **d**)

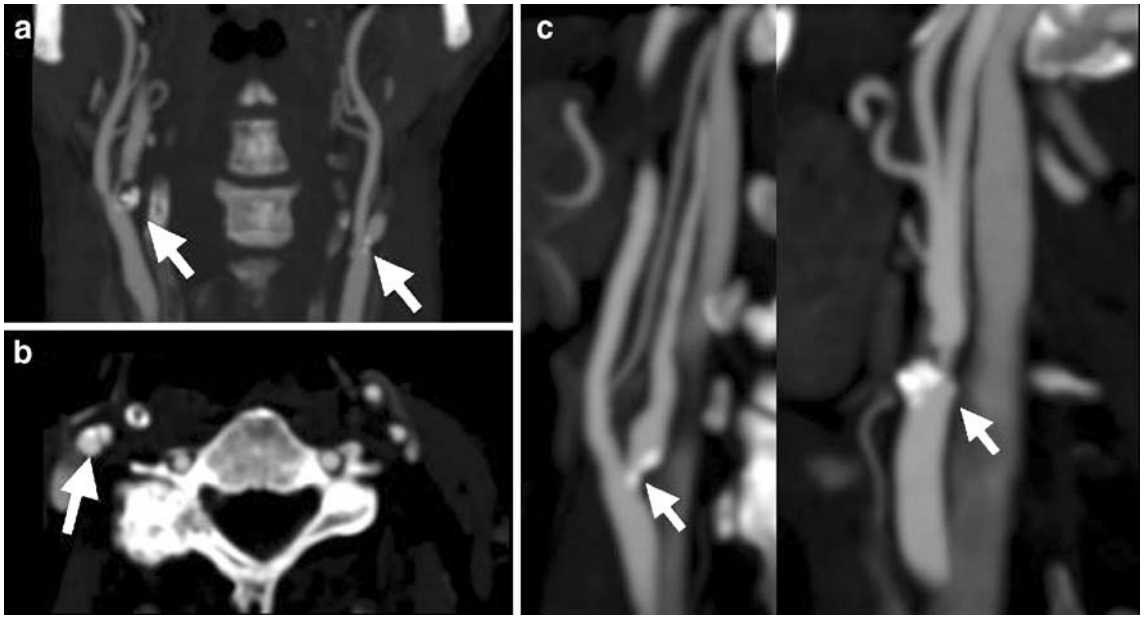

Fig. 19 Bilateral calcification and stenoses (*arrows*) of the carotid arteries, seen in the coronal (**a**), axial (**b**) and sagittal (**c**) planes on angio-CT

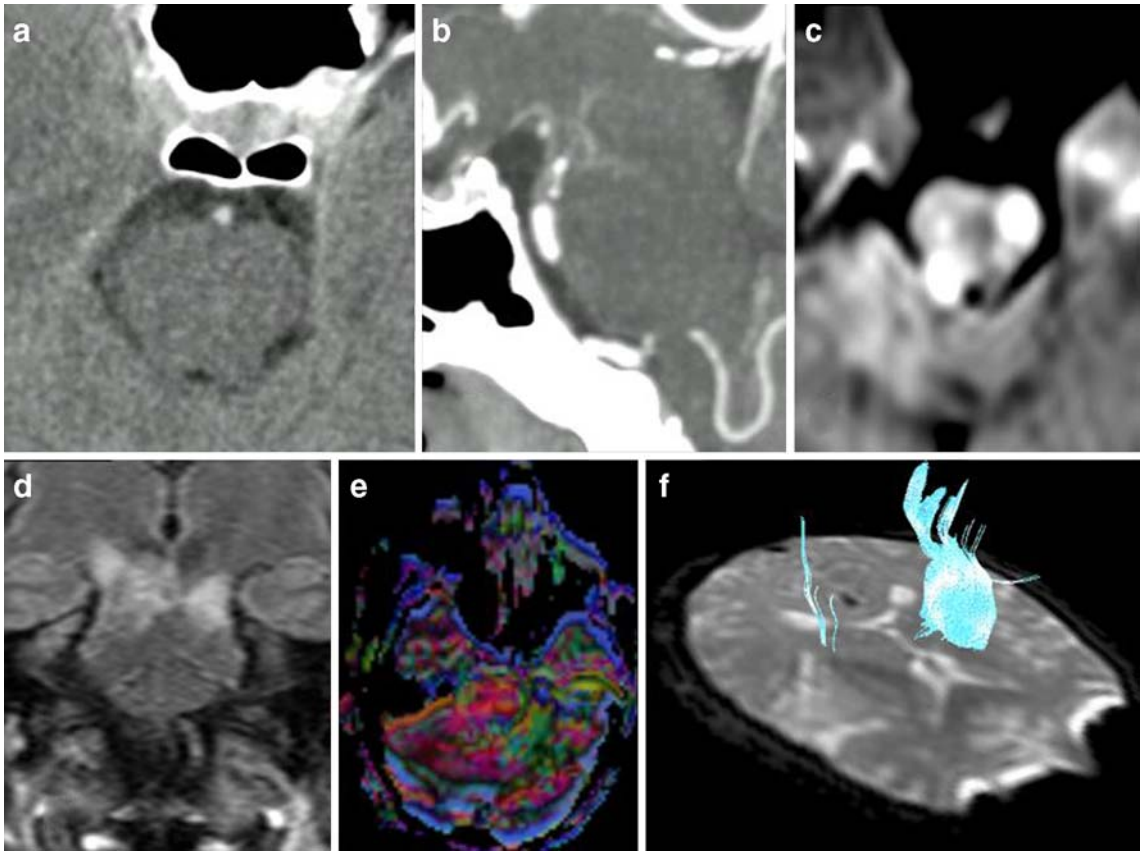

Fig. 20 Patient with basilar artery occlusion. Unenhanced CT shows hyperdensity of the basilar artery (**a**), and the angio-CT demonstrates the thrombus directly. The DWI image shows hyperintensities in the pons (**c**), seen bilaterally, more marked on the right, also on the FLAIR images. On the axial FA maps, there are low FA values in the pons (**d**), and the reconstructed tensor images show degeneration of the right-sided internal capsule (**f**)

hemorrhages [78]. The method employed should be able to direct the clinician and be able to demonstrate the possibility of proximal as well as distal vascular disease (Figs. 17, 18, 19).

Demonstration of the penumbra

Even though the exact definition of the penumbra has varied over the years since its original description [79], the ischemic penumbra corresponds to an ischemic brain region in a state of diminished cerebral blood flow that has not yet led to complete infarction and is potentially salvageable. It was believed to be situated between the thresholds for functional impairment and morphologic damage, and it is considered to be a dynamic process [80]. The penumbra in humans has been traditionally studied by nuclear medicine brain perfusion techniques such as positon emission tomography (PET) and single photon emission computed tomography (SPECT), but recently magnetic resonance imaging (MRI) techniques have also allowed us to gain insight into the mechanisms underlying ischemia. Traditionally, based on those cerebral blood flow studies, the ischemic penumbra has been defined as tissue with flow within the thresholds for maintenance of function and of morphologic integrity. The penumbra has recovery potential and therefore is the target for interventional therapy in acute ischemic stroke. It seems important to know that apparently early flow disturbances leading to rapid cellular damage are the major contributor to infarction, meaning that therapy should be targeted to the initially hypoperfused regions. More importantly, it has been demonstrated that functional imaging could represent a correlator for functional recovery after stroke or after thrombolysis. At first very motion-sensitive, functional MR techniques have entered a new age with the clinical introduction of echo-planar imaging, allowing such methods as diffusion- and perfusion-weighted MRI (DWI and PWI) to be performed more rapidly, therefore minimizing patient motion artifacts. In a proposed model, the so-called diffusion-perfusion mismatch represents the penumbra where the central diffusion defect at the initial time point corresponds to the penumbra and the surrounding hypoperfused area corresponds to a potential penumbra [81]. This model been proven useful in the clinical routine by further groups [82]. Other MR methods such as MR spectroscopy have also shown promise in the evaluation of the penumbra. Also, more advanced MR techniques based on the diffusion acquisition scheme such as diffusion tensor techniques are believed to show promise, especially since early changes in the tensor seem to accompany acute ischemia [83–90], and the tensor images eventually can demonstrate secondary Wallerian degeneration (Fig. 20).

Recently, due to the development of fast CT detectors, it has been possible to obtain stable perfusion maps of the brain. Using their model for the calculation of cerebral perfusion maps, Wintermark et al. found that, regarding the capacity to detect the penumbra in stroke patients, perfusion CT and MR diffusion and perfusion methods are equivalent [91].

Conclusion

Thanks to advances in MR and CT technology, it is now possible to image the brain and the whole neurovascular axis in a few minutes. This will help to contribute in a significant way to the treatment of acute cerebral ischemia. Indeed, while it is important to see what is or is not happening at the level of the cerebral parenchyma, the clinician involved in the diagnosis and management of stroke must also apprehend at an early stage what exactly the underlying cause of the ischemic lesion is. He or she therefore has to perform high-resolution imaging at the level of the cranio-cervical arteries. This will lead to the adoption of the so-called one-stop-shopping approach, where in one session, he or she will obtain not just the information on whether thrombolysis can be performed safely, but will also gain insight into possible proximal vascular or cardiac causes of the stroke. While it seems that MR technology together with diffusion imaging provides a more sensitive method that also provides more exact and objective data, CT has recently gained in acceptance [92].

When using MR methods, it will be necessary in the future also to use and evaluate all the parameters provided, not simply diffusion and perfusion imaging, but also to look in detail at the ADC maps in order to determine what is reversible and what is not, as well as to integrate findings from diffusion tensor images that could on the one hand go further into the penumbra and on the other hand provide insight into the re-organization of the ischemic brain by using the tractographic data also provided.

While on the one hand hemorrhage must be excluded, on the other, pathologies that can mimic stroke must be taken into account, such as venous thromboses. This can be done by performing an all-inclusive imaging protocol with both CT and MR technology.

However important these improvements in imaging quality might seem, it is extremely important not to forget to integrate further variables such as clinical scales and time to imaging into the whole picture. This led Baird and Warach to develop their three- and four-item scales that needed to be integrated into the evaluation of images in acute stroke patients before any therapeutic option could be evaluated [93, 94].

References

1. The National Institute of Neurological Disorders and Stroke rt-PA Stroke Study Group (1995) Tissue plasminogen activator for acute ischaemic stroke. N Engl J Med 333:1581–1587
2. Hacke W, Kaste M, Fieschi C, Toni D, Lesaffre E, von Kummer R, Boysen G, Bluhmki E, Hoxter G, Mahagne MH (1995) Intravenous thrombolysis with recombinant tissue plasminogen activator for acute hemispheric stroke. The European Cooperative Acute Stroke Study (ECASS). JAMA 274: 1017–1025
3. Hacke W, Kaste M, Fieschi C, von Kummer R, Davalos A, Meier D, Larrue V, Bluhmki E, Davis S, Donnan G, Schneider D, Diez-Tejedor E, Trouillas P (1998) Randomised double-blind placebo-controlled trial of thrombolytic therapy with intravenous alteplase in acute ischaemic stroke (ECASS II). Second European-Australasian Acute Stroke Study Investigators. Lancet 352(9136): 1245–1251
4. Gonner F, Remonda L, Mattle H, Sturzenegger M, Ozdoba C, Lovblad KO, Baumgartner R, Bassetti C, Schroth G (1998) Local intra-arterial thrombolysis in acute ischaemic stroke. Stroke 29:1894–1900
5. Furlan A, Higashida R, Wechsler L, Gent M, Rowley H, Kase C, Pessin M, Ahuja A, Callahan F, Clark WM, Silver F, Rivera F (1999) Intra-arterial prouro kinase for acute ischaemic stroke. The PROACT II study: a randomized controlled trial. Prolyse in acute cerebral thromboembolism. JAMA 282: 2003–2011
6. Arnold M, Schroth G, Nedeltchev K, Loher T, Remonda L, Stepper F, Sturzenegger M, Mattle HP (2002) Intra-arterial thrombolysis in 100 patients with acute stroke due to middle cerebral artery occlusion. Stroke 33 (7):1828–1833
7. Smith WS, Sung G, Starkman S, Saver JL, Kidwell CS, Gobin YP, Lutsep HL, Nesbit GM, Grobelny T, Rymer MM, Silverman IE, Higashida RT, Budzik RF, Marks MP; MERCI Trial Investigators (2005) Safety and efficacy of mechanical embolectomy in acute ischemic stroke: results of the MERCI trial. Stroke 36(7):1432–1438
8. Gobin YP, Starkman S, Duckwiler GR, Grobelny T, Kidwell CS, Jahan R, Pile-Spellman J, Segal A, Vinuela F, Saver JL (2004) MERCI 1: a phase 1 study of mechanical embolus removal in cerebral ischemia. Stroke 35(12): 2848–2854
9. Rovira A, Grive E, Rovira A, Alvarez-Sabin J (2005) Distribution territories and causative mechanisms of ischemic stroke. Eur Radiol 15(3):416–426
10. Vilela P, Goulao A (2005) Ischemic stroke: carotid and vertebral artery disease. Eur Radiol 15(3):427–433
11. Schellinger PD, Jansen O, Fiebach JB, Hacke W, Sartor K (1999) A standardized MRI stroke protocol: comparison with CT in hyperacute intracerebral haemorrhage. Stroke 30(4):765–768
12. Schellinger PD, Jansen O, Fiebach JB, Pohlers O, Ryssel H, Heiland S, Steiner T, Hacke W, Sartor K (2000) Feasibility and practicality of MR imaging of stroke in the management of hyperacute cerebral ischaemia. AJNR Am J Neuroradiol 21(7):1184–1189
13. Thurnher MM, Castillo M (2005) Imaging in acute stroke. Eur Radiol 15 (3):408–415
14. El-Koussy M, Guzman R, Bassetti C, Stepper F, Barth A, Lovblad KO, Schroth G (2000) CT and MRI in acute hemorrhagic stroke. Cerebrovasc Dis 10 (6):480–482
15. Patel MR, Edelman RR, Warach S (1996) Detection of hyperacute primary intraparenchymal haemorrhage by magnetic resonance imaging. Stroke 27 (12):2321–2324
16. Linfante I, Llinas RH, Caplan LR, Warach S (1999) MRI features of intracerebral haemorrhage within 2 hours from symptom onset. Stroke 30 (11):2263–2267
17. Atlas SW, Thulborn KR (1998) MR detection of hyperacute parenchymal haemorrhage of the brain. AJNR Am J Neuroradiol 19(8):1471–1477
18. Thulborn KR, Sorensen AG, Kowall NW, McKee A, Lai A, McKinstry RC, Moore J, Rosen BR, Brady TJ (1990) The role of ferritin and hemosiderin in the MR appearance of cerebral haemorrhage: a histopathologic biochemical study in rats. AJNR Am J Neuroradiol 11(2):291–297
19. Thulborn KR, Brady TJ (1989) Iron in magnetic resonance imaging of cerebral haemorrhage. Magn Reson Q 5(1): 23–38
20. Nighoghossian N, Hermier M, Adeleine P, Blanc-Lasserre K, Derex L, Honnorat J, Philippeau F, Dugor JF, Froment JC, Trouillas P (2002) Old microbleeds are a potential risk factor for cerebral bleeding after ischaemic stroke: a gradient-echo T2*-weighted brain MRI study. Stroke 33(3):735–742
21. Marks MP, Holmgren EB, Fox AJ, Patel S, von Kummer R, Froehlich (1999) Evaluation of early computed tomographic findings in acute ischemic stroke. Stroke 30(2):389–392
22. Unger E, Littlefield J, Gado M (1988) Water content and water structure in CT and MR signal changes: Possible influence in detection of early stroke. AJNR Am J Neuroradiol 9:687–691
23. von Kummer R, Holle R, Gizyska U, Hofmann E, Jansen O, Petersen D, Schumacher M, Sartor K (1996) Interobserver agreement in assessing early CT signs of middle cerebral artery infarction. AJNR Am J Neuroradiol 17 (9):1743
24. von Kummer R, Meyding-Lamadé U, Forsting M, Rosin L, Rieke K, Hacke W, Sartor K (1994) Sensitivity and prognostic value of early computed tomography in middle cerebral artery trunk occlusion. AJNR Am J Neuroradiol 15:9–15
25. von Kummer R, Bourquain H, Bastianello S, Bozzao L, Manelfe C, Meier D, Hacke W for the ECASS II Group (2001) Early prediction of irreversible brain damage after ischemic stroke by computed tomography. Radiology 219:95–100
26. von Kummer R, Allen KL, Holle R, Bozzao L, Bastianello S, Manelfe C, Bluhmki E, Ringleb P, Meier DH, Hacke W (1997) Acute stroke: usefulness of early CT findings before thrombolytic therapy. Radiology 205:327–333
27. Schuknecht B, Ratzka M, Hofmann E (1990) The “dense artery sign”-major cerebral artery thromboembolism demonstrated by computed tomography. Neuroradiology 32(2):98–103
28. Lövblad KO, Ozdoba C, Remonda L, Schroth G (1994) Computed tomography attenuation values in acute basilar occlusion. Cerebrovasc Dis 4:407–411

29. Gadda D, Vannucchi L, Niccolai F, Neri AT, Carmignani L, Pacini P (2005) Multidetector computed tomography of the head in acute stroke; predictive value of different patterns of the dense artery sign revealed by maximum intensity projection reformations for location and extent of the infarcted area. Eur Radiol 15(12):2387–2395
30. Yuh W, Crain M, Loes D, Greene G, Ryals T, Sato Y (1991) MR imaging of cerebral ischemia: Findings in the first 24 hours. AJNR Am J Neuroradiol 12:621–629
31. Kertesz A, Black S, Nicholson L, Carr T (1987) The sensitivity and specificity of MRI in stroke. Neurology 37: 1580–1585
32. Bryan N, Levy L, Whitlow W, Killian J, Preziosi T, Rosario J (1991) Diagnosis of acute cerebral infarction: Comparison of CT and MR Imaging. AJNR Am J Neuroradiol 12:611–620
33. Mohr J, Biller J, Hilal S, Yuh W, Tatemichi T, Hedges S, Tali E, Nguyen H, Mun I, Adams Jr H, Grisman K, Marler J (1995) Magnetic resonance versus computed tomographic imaging in acute stroke. Stroke 26:807–812
34. Edelman RR, Wielopolski P, Schmitt F (1994) Echo-planar MR imaging. Radiology 192(3):600–612
35. Le Bihan D, Breton E, Lallemand D, Grenier P, Cabanis E, Laval-Jeantet M (1986) MR Imaging of intravoxel incoherent motions: application to diffusion and perfusion in neurologic disorders. Radiology 161:401–407
36. Schlaug G, Siewert B, Benfield A, Edelman RR, Warach S (1997) Time course of the apparent diffusion coefficient (ADC) abnormality in human stroke. Neurology 49:113–119
37. Warach S, Chien D, Li W, Ronthal M, Edelman RR (1992) Fast magnetic resonance diffusion-weighted imaging of acute stroke. Neurology 42: 1717–1723
38. Chien D, Kwong KK, Gress DR, Buonanno FS, Buxton RB, Rosen BR (1992) MR diffusion imaging of cerebral infarction in humans. AJNR Am J Neuroradiol 13(4):1097–1102
39. Warach S, Gaa J, Siewert B, Wielopolski P, Edelman RR (1995) Acute human stroke studies by whole brain echo planar diffusion-weighted magnetic resonance imaging. Ann Neurol 37:231–241
40. Warach SJ, Dashe JF, Edelman RR (1996) Clinical outcome in ischemic stroke predicted by early diffusion-weighted and perfusion magnetic resonance imaging: A preliminary analysis. J Cereb Blood Flow Metab 16:53–59
41. Lövblad KO, Laubach HJ, Baird AE, Curtin F, Schlaug G, Edelman RR, Warach S (1998) Clinical experience with diffusion weighted MR in patients with acute stroke. AJNR 19:1061–1066
42. Gonzalez RG, Schaefer PW, Buonanno FS, Schwamm LH, Budzik RF, Rordorf G, Wang B, Sorensen AG, Koroshetz WJ (1999) Diffusion-weighted MR imaging: diagnostic accuracy in patients imaged within 6 h of stroke symptom onset. Radiology 210(1): 155–162
43. Yoneda Y, Tokui K, Hanihara T, Kitagaki H, Tabuchi M, Mori E (1999) Diffusion-weighted magnetic resonance imaging: detection of ischemic injury 39 minutes after onset in a stroke patient. Ann Neurol 45(6):794–797
44. Koroshetz WJ, Gonzalez G (1997) Diffusion-weighted MRI: an ECG for "brain attack"? Ann Neurol 41(5): 565–566
45. Mullins ME, Schaefer PW, Sorensen AG, Halpern EF, Ay H, He J, Koroshetz WJ, Gonzalez RG (2002) CT and conventional and diffusion-weighted MR imaging in acute stroke: study in 691 patients at presentation to the emergency department. Radiology 224 (2):353–360
46. Lansberg MG, Albers GW, Beaulieu C, Marks MP (2000) Comparison of diffusion-weighted MRI and CT in acute stroke. Neurology 25(8):1557–1561
47. Fiebach JB, Schellinger PD, Jansen O, Meyer M, Wilde P, Bender J, Schramm P, Juttler E, Oehler J, Hartmann M, Hahnel S, Knauth M, Hacke W, Sartor K (2002) CT and diffusion-weighted MR imaging in randomized order: diffusion-weighted imaging results in higher accuracy and lower interrater variability in the diagnosis of hyperacute ischemic stroke. Stroke 33 (9):2206–2210
48. Taleb M, Lovblad KO, El-Koussy M, Guzman R, Bassetti C, Arnold M, Oswald H, Remonda L, Schroth G (2001) Reperfusion demonstrated by apparent diffusion coefficient mapping after local intra-arterial thrombolysis for ischaemic stroke. Neuroradiology 43(7):591–594
49. Marks MP, Tong DC, Beaulieu C, Albers GW, de Crespigny A, Moseley ME (1999) Evaluation of early reperfusion and IV tPA therapy using diffusion- and perfusion-weighted MRI. Neurology 52:1792–1798
50. Kidwell CS, Saver JL, Mattiello J, Starkman S, Vinuela F, Duckwiler G, Gobin YP, Jahan R, Vespa P, Kalafut M, Alger JR (2000) Thrombolytic reversal of acute human cerebral ischemic injury shown by diffusion/perfusion magnetic resonance imaging. Ann Neurol 47:462–469
51. Lansberg MG, Tong DC, Norbash AM, Yenari MA, Moseley ME (1999) Intra-arterial rtPA treatment of stroke assessed by diffusion- and perfusion-weighted MRI. Stroke 30:678–680
52. Schellinger PD, Jansen O, Fiebach JB, Heiland S, Steiner T, Schwab S, Pohlers O, Ryssel H, Sartor K, Hacke W (2000) Monitoring intravenous recombinant plasminogen activator thrombolysis for acute ischemic stroke with diffusion and perfusion MRI. Stroke 31:1318–1328
53. Jansen O, Schellinger P, Fiebach J, Hacke W, Sartor K (1999) Early recanalisation in acute ischaemic stroke saves tissue at risk defined by MRI. Lancet 353:2036–2037
54. Oppenheim C, Grandin C, Samson Y, Smith A, Duprez T, Marsault C, Cosnard G (2001) Is there an apparent diffusion coefficient threshold in predicting tissue viability in hyperacute stroke? Stroke 32(11):2486–2491
55. Oppenheim C, Samson Y, Dormont D, Crozier S, Manai R, Rancurel G, Fredy D, Marsault C (2002) DWI prediction of symptomatic hemorrhagic transformation in acute MCA infarct. J Neuroradiol 29(1):6–13
56. Casey SO, Alberico RA, Patel M, Jimenez JM, Ozsvath RR, Maguire WM, Taylor ML (1996) Cerebral CT venography. Radiology 198:163–170
57. Lovblad KO, Schneider J, Bassetti C, El-Koussy M, Guzman R, Heid O, Remonda L, Schroth G (2002) Fast contrast-enhanced MR whole-brain venography. Neuroradiology 44(8):681–688
58. Lovblad KO, Bassetti C, Schneider J, Guzman R, El-Koussy M, Remonda L, Schroth G (2001) Diffusion-weighted MR in cerebral venous thrombosis. Cerebrovasc Dis 11(3):169–176
59. Ay H, Buonanno FS, Rordorf G, Schaefer PW, Schwamm LH, Wu O, Gonzalez RG, Yamada K, Sorensen GA, Koroshetz WJ (1999) Normal diffusion-weighted MRI during stroke-like deficits. Neurology 10:1784–1792
60. Oppenheim C, Stanescu R, Dormont D, Crozier S, Marro B, Samson Y, Rancurel G, Marsault C (2000) False-negative diffusion-weighted MR findings in acute ischemic stroke. AJNR Am J Neuroradiol 21:1434–1440
61. Kidwell C, Alger J, Di Salle F, Starkman S, Villablanca P, Bentson J, Saver J (1999) Diffusion MRI in patients with transient ischemic attacks. Stroke 30:1174–1180
62. Senn P, Lovblad KO, Zutter D, Bassetti C, Zeller O, Donati F, Schroth G (2003) Changes on diffusion-weighted MRI with focal motor status epilepticus: case report. Neuroradiology 45(4):246–249

63. Le Bihan D (1992) Theoretical principles of perfusion imaging Application to magnetic resonance imaging. Invest Radiol 27:6–11
64. Rosen BR, Belliveau JW, Vevea JM, Brady TJ (1990) Perfusion Imaging with NMR contrast agents. Magn Reson Med 14:249–265
65. Ostergaard L, Weisskoff RM, Chesler DA, Gyldensted C, Rosen BR (1996) High resolution measurement of cerebral blood flow using intravascular tracer bolus passages. Part I: Mathematical approach and statistical analysis. Magn Reson Med 36:715–725
66. Ostergaard L, Sorensen AG, Kwong KK, Weisskoff RM, Gyldensted C, Rosen BR (1996) High resolution measurement of cerebral blood flow using intravascular tracer bolus passages. Part II: Experimental comparison and preliminary results. Magn Reson Med 36:726–736
67. Edelman RR, Siewert B, Darby DG, Thangaraj V, Nobre AC, Mesulam MM, Warach S (1994) Qualitative mapping of cerebral blood flow and functional localization with echo-planar MR imaging and signal targeting with alternating radio frequency. Radiology 192(2):513–520
68. Chen Q, Siewert B, Bly BM, Warach S, Edelman RR (1997) STAR-HASTE: perfusion imaging without magnetic susceptibility artifact. Magn Reson Med 38(3):404–408
69. Siewert B, Schlaug G, Edelman RR, Warach S (1997) Comparison of EPISTAR and T2*-weighted gadolinium-enhanced perfusion imaging in patients with acute cerebral ischemia. Neurology 48(3):673–679
70. Sorensen AG, Copen WA, Ostergaard L, Buonanno FS, Gonzalez RG, Rordorf G, Rosen BR, Schwamm LH, Weisskoff RM, Koroshetz WJ (1999) Hyperacute stroke: simultaneous measurement of relative cerebral blood volume, relative cerebral blood flow, and mean tissue transit time. Radiology 210:519–527
71. Heid O (2000) T1-gewichtete MR Perfusion. Dissertation, University of Bern, Switzerland
72. Warach S, Wielopolski P, Edelman RR (1993) Identification and characterization of the ischemic penumbra of acute human stroke using echo planar diffusion and perfusion imaging. In: Proceedings of the 12th annual meeting of the Society of Magnetic Resonance in Medicine, Berkeley, Ca:263
73. Wintermark M, Maeder P, Thiran JP, Schnyder P, Meuli R (2001) Quantitative assessment of regional cerebral blood flows by perfusion CT studies at low injection rates: a critical review of the underlying theoretical models. Eur Radiol 11(7):1220–1230
74. Wintermark M, Thiran JP, Maeder P, Schnyder P, Meuli R (2001) Simultaneous measurement of regional cerebral blood flow by perfusion CT and stable xenon CT: a validation study. AJNR Am J Neuroradiol 22(5):905–914
75. Wintermark M, Fischbein NJ, Smith WS, Ko NU, Quist M, Dillon WP (2005) Accuracy of dynamic perfusion CT with deconvolution in detecting acute hemispheric stroke. AJNR Am J Neuroradiol 26(1):104–112
76. Remonda L, Heid O, Schroth G (1998) Carotid artery stenosis, occlusion, and pseudo-occlusion: first-pass, gadolinium-enhanced, three-dimensional MR angiography-preliminary study. Radiology 209(1):95–102
77. Remonda L, Senn P, Barth A, Arnold M, Lovblad KO, Schroth G (2002) Contrast-enhanced 3D MR angiography of the carotid artery: comparison with conventional digital subtraction angiography. AJNR Am J Neuroradiol 23(2):213–219
78. Sims JR, Rordorf G, Smith EE, Koroshetz WJ, Lev MH, Buonanno F, Schwamm LH (2005) Arterial occlusion revealed by CT angiography predicts NIH stroke score and acute outcomes after IV tPA treatment. AJNR Am J Neuroradiol 26(2):246–251
79. Astrup J, Siesjo BK, Symon L (1981) Thresholds in cerebral ischemia - the ischemic penumbra. Stroke 12:723–725
80. Heiss WD (2000) Ischemic penumbra: evidence from functional imaging in man. Cereb Blood Flow Metab 20 (9):1276–1293
81. Schlaug G, Benfield A, Baird A, Siewert B, Lövblad K, Parker R, Edelman RR, Warach S (1999) The ischemic penumbra of human stroke: using functional MRI parameters to define tissue at risk for infarct progression. Neurology 53:1528–1537
82. Ostergaard L, Sorensen AG, Chesler DA, Weisskoff RM, Koroshetz WJ, Wu O, Gyldensted C, Rosen BR (2000) Combined diffusion-weighted and perfusion-weighted flow heterogeneity magnetic resonance imaging in acute stroke. Stroke 31:1097–1103
83. Sorensen AG, Wu O, Copen WA, Davis TL, Gonzalez RG, Koroshetz WJ, Reese TG, Rosen BR, Wedeen VJ, Weisskoff RM (1999) Human acute cerebral ischemia: detection of changes in water diffusion anisotropy by using MR imaging. Radiology 212:785–792
84. Lovblad KO (2002) Diffusion-weighted MRI: back to the future. Stroke 33(9):2204–2205
85. Lovblad KO, Federspiel A, Oswald H, Kiefer C, Schroth G, Mattle H (2002) Diffusionstensorbildgebung der ischämichen Penumbra. Schweiz Med Forum 41:982–985
86. Lovblad KO, Kiefer C, Oswald H, Arnold M, Nedeltchev K, Mattle H, Schroth G (2003) Imaging the ischemic penumbra. Rivista di Neuroradiologia 16:833–838
87. Lövblad KO (2004) Neuroimaging of the ischemic penumbra. Schweizer Archiv für Neurologie und Psychiatrie 155:309–314
88. Lovblad KO, El-Koussy M, Oswald H, Baird AE, Schroth G, Mattle H (2004) Magnetic resonance imaging of the ischemic penumbra. Swiss Medical Weekly 133:551–559
89. Lövblad KO (2005) Magnetic resonance of the ischemic penumbra. Neurosci Imaging 1:85–88
90. Huisman TA (2003) Diffusion-weighted imaging: basic concepts and application in cerebral stroke and head trauma. Eur Radiol 13(10):2283–2297
91. Wintermark M, Reichhart M, Cuisenaire O, Maeder P, Thiran JP, Schnyder P, Bogousslavsky J, Meuli R (2002) Comparison of admission perfusion computed tomography and qualitative diffusion- and perfusion-weighted magnetic resonance imaging in acute stroke patients. Stroke 33 (8):2025–2031
92. Koroshetz WJ, Gonzalez G (1999) Imaging stroke in progress: Magnetic resonance advances but computed tomography is poised for counterattack. Ann Neurol 46:556–558
93. Baird AE, Dambrosia J, Janket S, Eichbaum Q, Chaves C, Silver B, Barber PA, Parsons M, Darby D, Davis S, Caplan LR, Edelman RE, Warach S (2001) A three-item scale for the early prediction of stroke recovery. Lancet 357(9274):2095–2099
94. Steven Warach (2001) Tissue viability thresholds in acute stroke. The 4-factor model. Stroke 32:2460